

Transesterification of Tributyrin and Dehydration of Fructose over a Carbon-Based Solid Acid Prepared by Carbonization and Sulfonation of Glucose

Chuanxu Wang,^[a] Fulong Yuan,^[a] Lijing Liu,^[a] Xiaoyu Niu,^{*,[b]} and Yujun Zhu^{*,[a]}

A series of carbon-based sulfonated solid acid (CS) catalysts can be prepared through a facile method of direct simultaneous carbonization and sulfonation of D-glucose with concentrated sulfuric acid without a hydrothermal process. Temperature is a key factor in obtaining CS catalysts with higher amounts of -SO₃H acid sites. The transesterification of tributyrin with methanol and the dehydration of fructose to 5-hydroxymethylfurfural (5-HMF) are investigated over the CS catalysts. The CS-150 catalyst, which is the CS catalyst prepared at

150 °C, shows much higher catalytic activity to give a tributyrin conversion of 99.4%. The yield of methyl butyrate is 97.2% and a remarkably high yield of 5-HMF (93%) can be obtained efficiently; these yields result from the high acid density of -SO₃H. Good linearity is displayed between the total acid density and yield of methyl butyrate/5-HMF. The CS-150 catalyst has high stability and good recyclability for the dehydration of fructose.

Introduction

With growing concerns about energy consumption and issues of environmental pollution, the utilization of environmentally friendly catalytic materials has become a top priority in the chemical industry.^[1] In recent decades, acid-catalyzed reactions, such as transesterification and dehydration of carbohydrates, have attracted much attention in the production of chemicals.^[2] Most acid-catalyzed processes are performed in the presence of homogeneous acids, such as H₂SO₄, H₃PO₄, and HCl; however, corrosion, toxicity, and separation problems limit their industrial application.^[3] With the development of catalytic science and advances in environmental awareness, searching for recoverable and reusable solid acid catalysts to replace homogeneous acid catalysts has become a hot research field. To date, several researchers have reported a variety of solid acid catalysts, such as zeolites, resins, oxides, and phosphates,^[4] for the production of a variety of chemical products.^[5]

In recent years, with research into carbon materials, sulfonated carbon materials have shown promising applications as new, cheap, and environmentally friendly solid acid catalysts. One type of sulfonated carbon catalyst was prepared by pyrolytic treatment of biomass feeds under hydrothermal condi-

tions and subsequent sulfonation. These SO₃H-bearing carbons exhibited remarkable catalytic properties for various acid-catalyzed reactions, such as esterification, transesterification, hydration, hydrolysis, and dehydration of sugars.^[3c,4d,5c] Hara et al. prepared a carbon-based solid acid by incomplete carbonization of sulfonated aromatic compounds.^[6] Later, they prepared sulfonated carbon by the sulfonation of incompletely carbonized sugars and proved that the activity was comparable to that of liquid sulfuric acid in the esterification of higher fatty acids.^[7] The particular amorphous carbon materials with SO₃H groups were also considered as new types of solid acids,^[3b] these exhibited remarkable catalytic performances for various acid-catalyzed reactions, such as the esterification of higher fatty acids,^[7] hydration,^[8] and hydrolysis.^[9] There are two routes for the preparation of amorphous carbon with SO₃H groups: incomplete carbonization of sulfoaromatic compounds^[6] and sulfonation of incompletely carbonized organic matter.^[8,9] Fraile and co-workers reported that sulfonated hydrothermal carbons were highly active for esterification of palmitic acid with different alcohols.^[10] Qi et al. prepared cellulose-derived carbonaceous solids by hydrothermal carbonization of cellulose followed by sulfonation. The obtained carbonaceous solid acids exhibited good activity in fructose dehydration to give 5-hydroxymethylfurfural (5-HMF).^[11] Recently, Ji et al. prepared a sulfonated graphene acid catalyst that had high catalytic activity and could be repeatedly used as a water-tolerant solid acid catalyst.^[12] Xiao's group also demonstrated a facile synthesis of sulfated graphene (G-SO₃H) from hydrothermal sulfonation by using fuming sulfuric acid at a relatively high temperature (180 °C).^[13] More importantly, G-SO₃H exhibited much better activity and recyclability. In addition, a series of sulfonic acid functionalized carbon materials, including poly(*p*-styrene-sulfonic acid)-grafted carbon nanotubes (CNT-PSSA), poly(*p*-

[a] C. Wang, Prof. F. Yuan, L. Liu, Prof. Y. Zhu
Key Laboratory of Functional Inorganic Material Chemistry
Ministry of Education School of Chemistry and Materials
Heilongjiang University, 74 Xuefu Road, Harbin 150080 (P. R. China)
E-mail: yujunzhu@hlju.edu.cn

[b] Dr. X. Niu
Key Laboratory of Chemical Engineering Process
& Technology for High-efficiency Conversion
College of Heilongjiang Province, School of Chemistry and Materials
Heilongjiang University, Harbin 150080 (P. R. China)
E-mail: niuxiaoyu2000@126.com

Supporting information for this article is available on the WWW under
<http://dx.doi.org/10.1002/cplu.201500261>.

styrenesulfonic acid)-grafted carbon nanofibers (CNF-PSSA), benzenesulfonic acid grafted CMK-5 (CMK-5-BSA), and benzenesulfonic acid grafted carbon nanotubes (CNT-BSA), have been studied for fructose dehydration to give 5-HMF and fructose alcoholysis to give alkyl levulinate.^[14] Sulfonated carbon nanotubes and porous carbon also displayed significant activities as acid catalysts owing to high acidities and -SO₃H densities.^[15] However, it must be pointed out that the methods to prepare the above-mentioned carbon-based solid acids are complex and expensive; thus, it is interesting to explore a novel facile synthetic method for carbon-based solid acids with high catalytic activities and low costs.

Herein, we report on a one-pot, facile synthetic method for a carbon-based solid acid (CS) catalyst by direct simultaneous carbonization and sulfonation, without a hydrothermal process, with glucose and concentrated sulfuric acid as raw materials. The obtained catalyst has a high acid density and acid strength; moreover, it is low cost. Their catalytic performances have been investigated by using the transesterification of tributyrin with methanol to give methyl butyrate and the dehydration of fructose to give 5-HMF as model reactions. Various parameters, such as reaction temperature, time, and ratio of glucose to H₂SO₄, were varied to optimize the preparation conditions to achieve a solid acid catalyst with much higher activity by using transesterification of tributyrin as a probe reaction. Among these synthetic conditions, temperature plays a key role in the formation of CS catalyst with much higher acid site density, resulting in higher activity for the direct simultaneous carbonization and sulfonation of glucose with H₂SO₄.

Results and Discussion

The CS catalysts were prepared, without using a hydrothermal process, by direct simultaneous carbonization and sulfonation with glucose and concentrated sulfuric acid as raw materials in a low-cost, facile synthetic process. To achieve a CS catalyst with much higher activity, the effects of various preparation parameters, such as reaction temperature, time, and ratio of glucose to H₂SO₄, on the catalytic activity were optimized by using the transesterification of tributyrin with methanol as a model reaction. The optimized synthetic conditions involved a carbonization and sulfonation time of 20 min (Figure S1 in the Supporting Information) and a ratio of the amount of glucose (g) to H₂SO₄ volume (mL) of 1:6 (Figure S2 in the Support-

ing Information). Among the various synthetic conditions investigated, temperature plays a key role in the formation of a CS catalyst with a much higher acid site density. Thus, herein, we describe in detail the effect of different preparation temperatures on the catalytic performance of CS catalysts. The CS catalysts were prepared at 130, 150, and 170 °C, and are denoted as CS-130, CS-150, and CS-170, respectively, hereafter.

Figure 1 shows the XRD patterns of the CS-*T* (*T* = 130, 150, and 170 °C) catalysts. All XRD patterns exhibit a broad diffraction peak in the 2θ range of 15 to 37° that is assigned to the C(002) plane of the amorphous carbon composed of aromatic carbon. The C(101) plane, which gives rise to a weak and broad diffraction peak at 37–50°, can be distinguished in these samples, although it is not clear. This peak is attributed to the axis of the graphite structure.^[16] As a result of these two peaks, we can deduce that the CS catalysts consist of a carbon sheet and amorphous carbon with aromatic carbon rings.

Table 1 shows the elemental composition of the CS catalysts. The carbon content is about 57% for the CS-130, CS-150, and CS-170 catalysts; moreover, the ratio of carbon to hydrogen is above 1.35 for these CS catalysts. The amount of sulfur is 3.890, 4.081, and 2.960% for CS-130, CS-150, and CS-170, respectively. The sulfur content decreases in the following order: CS-150 > CS-130 > CS-170. It is noted that about 36% of the composition is oxygen, which indicates that some oxygen-containing groups may be formed during the preparation process. Based on the elemental analysis results, the elemental composition is CH_{0.74}O_{0.47}S_{0.026}, CH_{0.69}O_{0.47}S_{0.027}, and CH_{0.62}O_{0.49}S_{0.019} for

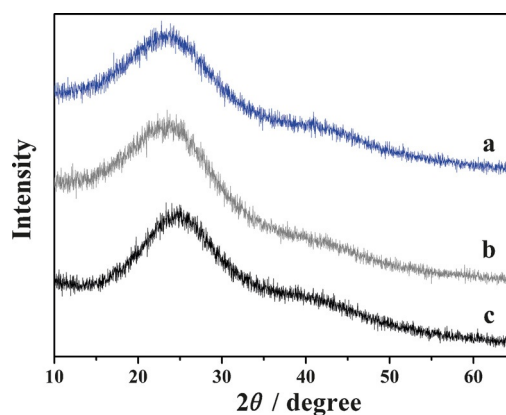


Figure 1. XRD patterns of the CS catalysts: a) CS-130, b) CS-150, and c) CS-170.

Table 1. Texture properties of the CS catalysts.

Catalyst	BET surface area [m ² g ⁻¹]	<i>I_D</i> / <i>I_G</i> ^[a]	Element composition [%]				Acid site density [mmol g ⁻¹]	total		
			C	H	S	O		atomic ratio	H ⁺ (SO ₃ H)	H ⁺ (other)
CS-130	11.0	0.86	57.05	3.498	3.890	35.56	CH _{0.74} O _{0.47} S _{0.026}	1.22	0.14	1.36
CS-150	9.2	0.80	56.92	3.270	4.081	35.73	CH _{0.69} O _{0.47} S _{0.027}	1.28	0.31	1.59
CS-170	8.4	0.75	57.12	2.955	2.960	36.96	CH _{0.62} O _{0.49} S _{0.019}	0.92	0.40	1.32
used CS-150 ^[b]	7.8	0.78	55.28	2.551	2.298	39.87	CH _{0.55} O _{0.54} S _{0.015}	0.71	0.02	0.73
used CS-150 ^[c]	8.7	0.81	56.78	3.305	3.986	35.93	CH _{0.70} O _{0.47} S _{0.026}	1.25	0.30	1.55

[a] Data from Raman spectra; *I_D*/*I_G* is the intensity ratio of the D band to G band. [b] For the transesterification of tributyrin with methanol after one cycle. [c] For the dehydration of fructose to 5-HMF after three cycles.

CS-130, CS-150, and CS-170, respectively. Combined with the results from XRD, these results suggest that the structure of the CS catalyst may include an incompletely carbonized carbon sheet with aromatic carbon rings.

Raman spectroscopy was used to investigate the degree of crystallinity of the carbon materials. For the CS catalysts, two prominent bands can be observed in Figure 2, at $\tilde{\nu} \approx 1365$ and 1590 cm^{-1} , which are usually assigned to the breathing mode

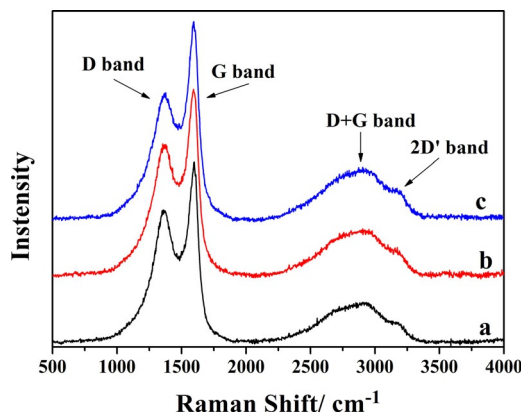


Figure 2. Raman spectra of the CS catalysts: a) CS-130, b) CS-150, and c) CS-170.

of κ -point phonons of A_{1g} symmetry and the E_{2g} phonons of sp^2 -carbon atoms, respectively.^[12,17] The band at $\tilde{\nu} \approx 1590 \text{ cm}^{-1}$ is attributable to the G band commonly observed in graphitic materials. The band at $\tilde{\nu} = 1365 \text{ cm}^{-1}$ is assigned to the D band, which is commonly associated with the presence of defects in the graphite layer.^[3b] It is well known that an increase in the intensity ratio of the D band to G band (I_D/I_G) indicates a decrease in the graphite crystallinity of the carbon materials.^[18] In our case, the I_D/I_G values for the CS-130, CS-150, and CS-170 samples are 0.86, 0.80, and 0.75, respectively (Table 1). The results suggest that the obtained CS samples have a poor degree of crystallinity and carbonation, which is in agreement with XRD analyses. The higher I_D/I_G with increasing preparation temperature results in a lower degree of graphitization and carbonation. It can be deduced that temperature has a greater impact on the degree of carbonization of the CS catalysts.

FTIR spectroscopy was employed as an additional probe to provide evidence for the presence of $-\text{SO}_3\text{H}$ groups and other organic species in the CS catalysts (Figure 3). It is clear that the IR spectra of the CS catalysts (Figure 3a–c) have undergone drastic changes compared with glucose (Figure 3d). The vibration bands at $\tilde{\nu} = 1701$ and 1623 cm^{-1} in Figure 3a–c are attributed to the stretching vibrations of C=O in the carboxylic acid^[19] and C=C in the aromatic ring,^[10] respectively. This indicates that glucose is carbonized through dehydration with concentrated sulfuric acid at different temperatures. The broad absorption band at $\tilde{\nu} = 1250$ – 1150 cm^{-1} and the sharp band at $\tilde{\nu} = 1030 \text{ cm}^{-1}$ are assigned to the asymmetric and symmetric stretching vibrations, respectively, of the SO_2 group of the CS

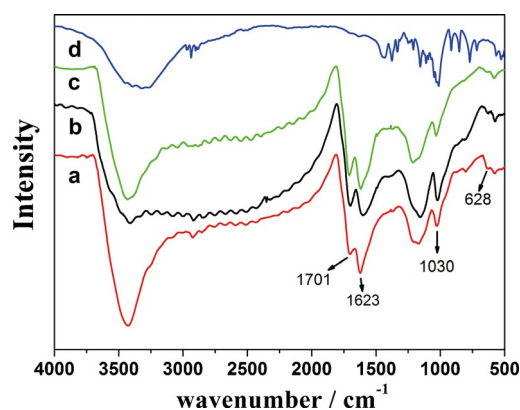


Figure 3. FTIR spectra of the CS catalysts: a) CS-130, b) CS-150, c) CS-170, and d) glucose.

samples.^[20] The band at $\tilde{\nu} = 628 \text{ cm}^{-1}$ is attributed to vibration of the C–S bond.^[21] The results indicate that the carbonation reaction proceeds simultaneously with sulfonation. In other words, sulfonic groups can be formed to accompany the carbonation of glucose. The thermal decomposition experiments also prove these results. Figure 4 displays the results of temperature-programmed decomposition of the CS-150 catalyst. The results indicate that the peak at 206°C can be assigned to the formation of SO_2 , namely, the decomposition of the sulfonic acid group on the surface of the CS-150 catalyst. This confirms that the sulfonic acid group can be grafted onto the surface of the CS catalysts and remain stable below 206°C in air.

The results from elemental analysis, XRD, Raman spectroscopy, and IR spectroscopy verify that the structure of the CS catalyst is composed of an incompletely carbonized carbon sheet and amorphous carbon containing aromatic carbon rings with sulfonic acid groups ($-\text{SO}_3\text{H}$).

Table 1 shows the surface acidity of the CS catalysts. The total acid-site density of the CS samples was estimated by the acid–base titration method, and the content of $-\text{SO}_3\text{H}$ was calculated by elemental analysis based on the sulfur component. The other H^+ amount is that of the difference between the

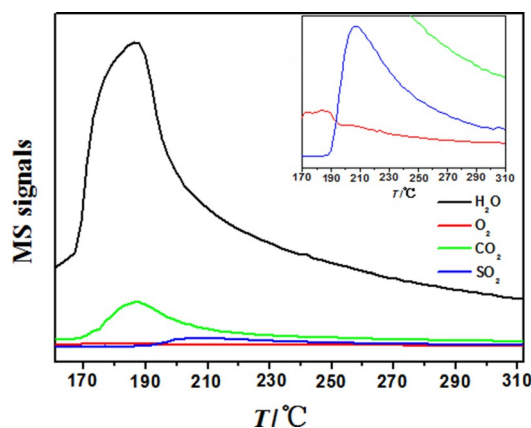


Figure 4. Spectrum obtained by temperature-programmed decomposition of the CS-150 catalyst.

acid-site density and $-SO_3H$ content. The total acid-site density is 1.36, 1.59, and 1.32 $mmol\ g^{-1}$ for CS-130, CS-150, and CS-170, respectively. Accordingly, the amount of SO_3H is 1.22, 1.28, and 0.92 $mmol\ g^{-1}$, respectively. The amount of $-SO_3H$ groups dominates the total acid-site density for the CS samples; meanwhile, the CS-150 catalyst possesses the highest concentration of sulfonic groups. For the CS-170 sample, the amount of $-SO_3H$ is low, which may be attributed to the enhanced degree of carbonization, leading to hydrolysis of the sulfonic acid groups by water produced during the carbonation process because the temperature ($170^\circ C$) is too high. The amount of other H^+ acid increases from 0.14 $mmol\ g^{-1}$ to 0.31 and 0.40 $mmol\ g^{-1}$ for the CS-130, CS-150, and CS-170 catalysts, which reveals that more $-OH$ and $-COOH$ groups are formed when the temperature increases from 130 to $170^\circ C$. However, the amount of acid of the other H^+ from $-OH$ and $-COOH$ groups is clearly less than the amount of $-SO_3H$. This demonstrates that the acidity of the CS catalysts is derived from the SO_3H groups. The results indicate that the appropriate preparation temperature should be selected to obtain a CS catalyst with the highest acid density.

The above results indicate that the prepared CS catalysts possess the characteristics of amorphous carbon with a high acid-site density of SO_3H groups. In particular, the CS-150 catalyst exhibits the highest acid-site density.

The hydrophobic and lipophilic properties of the CS catalysts were measured. Figure 5 gives the results from contact-angle (CA) measurements for the CS catalysts. From CA data for water ($CA \approx 142^\circ$; Figure 5a1–3), the CS catalysts are poorly hydrophilic. In comparison with results for the lipophilicity (Figure 5b1–3, the CA of all CS catalysts is approximately 0° , which indicates that the CS samples have good lipophilicity properties.

Figure 6 shows the transesterification of tributyrin with methanol over the CS catalysts. High catalytic activities were

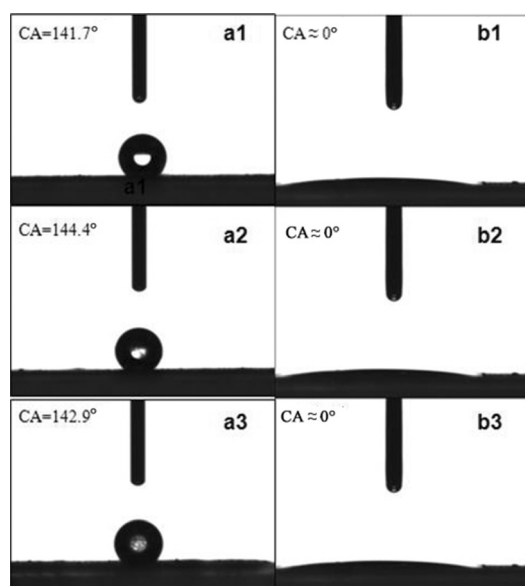


Figure 5. Contact angles of a) a water droplet and b) a soybean oil droplet on the catalyst surface: a1,b1) CS-130; a2,b2) CS-150; and a3,b3) CS-170.

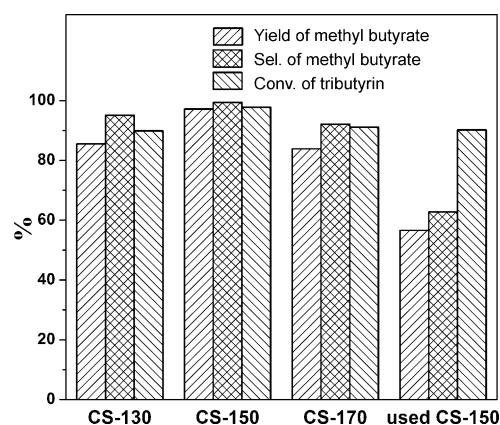


Figure 6. Activity of the transesterification of tributyrin with methanol over the CS catalysts; 20 mg of catalyst, ratio of catalyst to tributyrin is 20 ($mg\ g^{-1}$), molar ratio of methanol to tributyrin is 20:1, reaction temperature $80^\circ C$, reaction time 8 h.

obtained for this reaction, although the BET surface area was low as $8.4\text{--}11.0\ m^2\ g^{-1}$ (Table 1). Over 95% tributyrin conversion and nearly 85% yield of methyl butyrate could be obtained with all CS catalysts. In particular, 97.8% selectivity and 97.2% yield of methyl butyrate were obtained with the CS-150 sample; this corresponded to 99.4% conversion of tributyrin. The effects of the various reaction conditions, including temperature, reaction time, molar ratio of methanol to tributyrin, and the amount of catalyst, on the activity were also investigated for the CS-150 catalyst based on its good catalytic activity. The results are presented in Figures S3–S6 in the Supporting Information, and suggest that the CS-150 catalyst shows excellent catalytic performance for the transesterification of tributyrin in a 20:1 molar ratio of methanol to tributyrin with 20 mg of catalyst and 1.0 g of tributyrin at $80^\circ C$ for 8 h.

Figure 7 is a plot of the yield of methyl butyrate versus the total acid density for the CS catalysts in Table 1. The results reveal good linearity between the yield of methyl butyrate and the total acid density of the CS catalysts. According to the order from CS-170 to CS-130 and CS-150, the total acid density increases, and the yield of methyl butyrate is also markedly en-

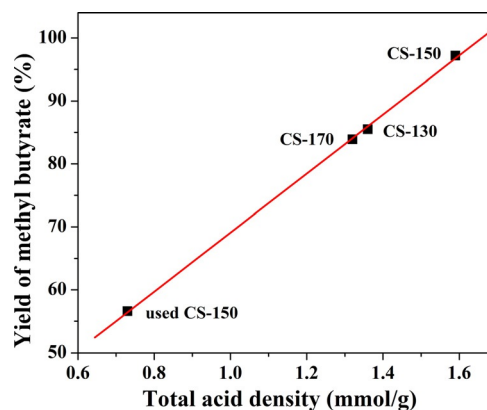


Figure 7. Plot of the yield of methyl butyrate versus total acid density for the CS catalysts.

hanced. These results prove that all of the surface protonated acids are the active acid sites of the CS catalysts for the transesterification of tributyrin with methanol. The sulfonic acid groups dominate the total acid density. Thus, the CS-150 catalyst, which has the highest concentration of sulfonic acid groups, is the most active catalyst for the transesterification of tributyrin with methanol. In addition, the lipophilicity of the CS catalysts leads to the enhanced local adsorption of tributyrin, which should promote the catalytic transesterification reaction.^[22] A similar result was reported by Wang et al.,^[23] who developed a carbon-based solid acid catalyst through the sulfonation of carbonized vegetable oil asphalt and petroleum asphalt. This carbon-based solid acid exhibited high catalytic activity for the simultaneous esterification and transesterification of a waste vegetable oil containing large amounts of free fatty acids. The high catalytic activity is ascribed to the high acid-site density.^[2a,23] Additionally, Keggin-type heteropolyacids, including $H_3PW_{12}O_{40}$, $H_4SiW_{12}O_{40}$, $H_3PMo_{12}O_{40}$, and $H_4SiMo_{12}O_{40}$, have been applied in the transesterification of rapeseed oil with methanol and ethanol, and they exhibit outstanding catalytic activity comparable to that of H_2SO_4 .^[2a] This excellent transesterification activity is explained in terms of the high acid strength of the heteropolyacids compared with that of H_2SO_4 . Thus, the CS catalyst, with the much higher concentration of $-SO_3H$, is favorable in the transesterification reaction.

Based on our previous studies and results reported in the literature,^[24] the transesterification reaction proceeds according to pseudo-first-order kinetics, and the kinetic model is given by Equation (1), where gives the yield of methyl butyrate at time t (min).

$$-\ln(1 - \text{yield}_{\text{methyl butyrate}}) = kt \quad (1)$$

A plot of $-\ln(1 - \text{yield}_{\text{methyl butyrate}})$ as a function of time will be linear, with a slope equal to the reaction rate constant, k .

The kinetics of the CS-150-catalyzed transesterification of tributyrin has been studied in the temperature range of 333–353 K. A graph of $-\ln(1 - \text{yield}_{\text{methyl butyrate}})$ versus t is given in Figure 8a. The plots are represented by straight lines, which validate the first-order reaction model. The rate constants were calculated from these plots and found to be 0.00317, 0.00441, and 0.00597 min^{-1} at 333, 343, and 353 K, respectively. The activation energy (E_a) and pre-exponential factor (A) for the same reaction were determined by the Arrhenius equation [Eq. (2)].

$$\ln k = -E_a/RT + \ln A \quad (2)$$

A plot of $\ln k$ versus $1/T$ is shown in Figure 8b. The slopes of the lines provide the activation energy (E_a) by using Equation (2); in this case, the activation energy calculated from the slope of the Arrhenius plot is 30.7 kJ mol^{-1} and the corresponding pre-exponential factor is 209 min^{-1} . The activation energy for the CS-150 solid acid catalyst is much lower than that of the 25% $KF/La_2O_2CO_3$ (55.03 kJ mol^{-1}) and KF/La_2O_3 (128.9 kJ mol^{-1}) solid base catalysts used in our previous study.^[25]

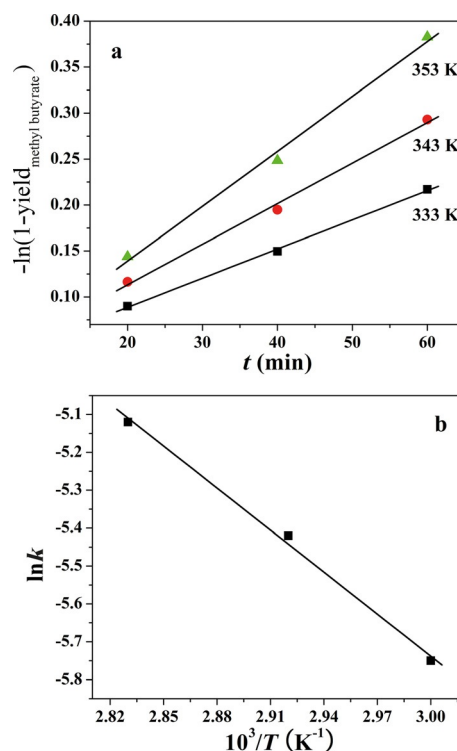
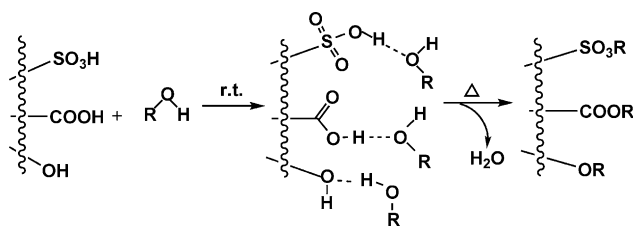


Figure 8. a) Plots of $-\ln(1 - \text{yield}_{\text{methyl butyrate}})$ versus time at different temperatures. b) Arrhenius plot of $\ln k$ versus $10^3/T$ for the reaction of tributyrin with methanol. Reaction conditions: 20 mg of CS-150 catalyst, the ratio of catalyst to tributyrin is 20 (mg g^{-1}), molar ratio of methanol to tributyrin = 20:1.

The reusability of the CS-150 catalyst has also been investigated and the results are depicted in Figure 6. The used CS-150 catalyst was separated from the reaction mixture by filtering and washing with methanol several times, and then reused under the same reaction conditions as the original reaction. The conversion of tributyrin decreased to 62.7%; however, the selectivity of methyl butyrate maintained a much higher value (90.2%). The yield of methyl butyrate decreased from 91.3 to 56.6%, which indicated that the catalyst was partially deactivated during the recycling process. The BET surface area ($7.8 \text{ m}^2 \text{ g}^{-1}$) and I_D/I_G value (0.78) obtained from the Raman spectra of the used CS-150 catalyst are not significantly changed compared with the fresh CS-150 catalyst (Table 1); however, the acid-site density of the used CS-150 catalyst decreases to 0.71 and 0.02 mmol g^{-1} for $H^+(SO_3H)$ and $H^+(\text{other})$, respectively, and a decrease of 0.86 mmol g^{-1} for the total acid-site density from fresh CS-150 to the used CS-150 catalyst (Table 1). It is interesting that the linear relationship is also present between the yield of methyl butyrate and the total acid-site density for the used CS-150 and fresh CS catalysts (Figure 7). Therefore, it can be concluded that the deactivation of the CS-150 catalyst is related to the loss of $H^+(SO_3H)$. The formation of sulfonate esters may account for the deactivation behavior in reactions taking place in alcohols as solvents, especially with methanol, owing to its higher reactivity. Fraile and co-workers reported a general picture of the interaction between $HC-SO_3H$ and alcohols (Scheme 1), in which the formation of hydrogen bonds was favored between the alcohol and



Scheme 1. Deactivation of the CS catalysts ($\text{R} = \text{CH}_3$).

protonated groups of different materials (sulfonic and carboxylic acids, hydroxyls of alcohols, and phenols) at room temperature.^[10] The formation of sulfonate esters through the sulfonic groups reacting with the alcohol at reaction temperature explains the strong deactivation effect of the CS-150. In other words, the CS-150 catalyst interacts with methanol, so the total acid-site density decreases under the reaction conditions. Thus, the catalytic activity of the reused CS-150 catalyst declined significantly in the transesterification of tributyrin with methanol.

The product 5-HMF is mainly synthesized by the acid-catalyzed dehydration of monosaccharides.^[2c,d,14] The dehydration of fructose is closely associated with the acidity of the catalyst, especially the acid sites.^[2d,14,26] Because the CS-150 catalyst exhibited the highest acid density and $\text{-SO}_3\text{H}$ concentration, as well as excellent acid catalysis performance for transesterification of tributyrin with methanol, the dehydration of fructose to 5-HMF was evaluated over the CS-150 catalyst. The effects of various reaction conditions, including temperature, time, and the amount of catalyst on the activity of the dehydration of fructose to 5-HMF, were investigated over the CS-150 catalyst. The results are presented in Figures 9–11 below. In addition to the effectiveness of the catalyst for high yield and highly selective HMF production, solvent, including water, isopropanol, sulfolane, and DMSO, also plays an important role in enhancing the HMF yield. DMSO can suppress undesired side reactions and increase the selectivity of 5-HMF.^[2c,d,27] Therefore, DMSO was used as the solvent in this study for the dehydration of fructose to give 5-HMF. The main byproducts of these reactions are humins. Currently, the humins cannot be quantified owing to their composition. Thus, the conversion of fructose, as well as the selectivity and yield of 5-HMF, were considered.

The effect of the amount of catalyst on the dehydration of fructose to 5-HMF was investigated over the CS-150 catalyst (Figure 9). The 5-HMF yield was 75% when the amount of CS-150 used was 10 mg. The yield of 5-HMF improved to 93% when the amount of catalyst was augmented to 30 mg. The increase in the yield of 5-HMF with the catalyst dosage could be attributed to an increase in the availability and number of active sites during the dehydration of fructose. However, a further increase in the amount of catalyst to 50 mg led to a slightly reduced 5-HMF yield of 87%; this indicated acid-catalyzed, rapid oligomerization of 5-HMF over the surface of the CS-150 catalyst under a higher acid-site concentration.^[14] Thus, a large amount of catalyst is not necessary to optimize the reaction.

The effect of the reaction time on the dehydration of fructose to 5-HMF over the CS-150 catalyst was investigated and

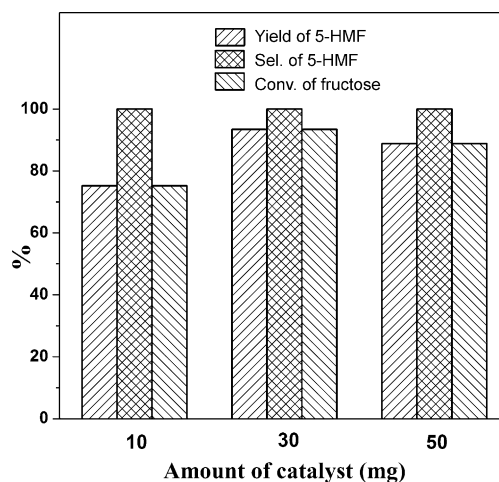


Figure 9. Effect of the amount of catalyst on the dehydration of fructose to 5-HMF over CS-150; reaction conditions: 200 mg of fructose, reaction time 30 min at 140 °C.

the results are depicted in Figure 10. The 5-HMF yield increased from 15 to 45 min and thereafter remained constant. The maximum 5-HMF yield (93%) was obtained at 140 °C after a reaction time of 30 min; prolonged reaction, however, led to a slight reduction in the yield of 5-HMF. Therefore, the results in Figure 10 show that 30 min is the optimum period to obtain a high yield of 5-HMF.

Figure 11 shows the influence of the reaction temperature in the range of 100 to 160 °C on the dehydration of fructose catalyzed by CS-150. The reaction temperature greatly affects the conversion of fructose and formation of 5-HMF. The conversion of fructose and selectivity of 5-HMF were 34 and 28% at 100 °C, respectively. Through increasing the temperature, the conversion sharply improved and nearly 100% conversion of fructose was achieved at 120 °C and thereafter remained constant. The yield of 5-HMF was only 9.6% at 100 °C, whereas it increased quickly to 83% at 120 °C; this confirmed that increas-

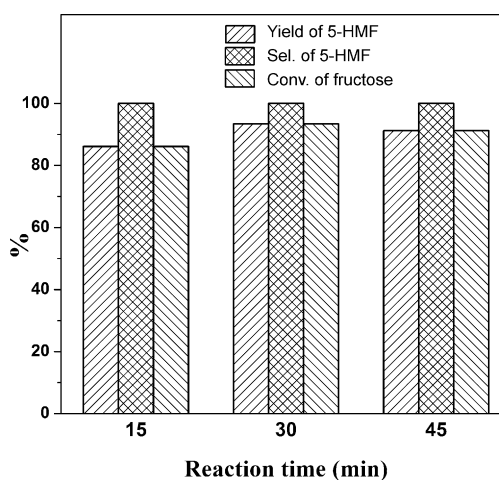


Figure 10. Effect of reaction time on the dehydration of fructose to 5-HMF over CS-150; reaction conditions: 200 mg of fructose, 30 mg of CS-150, at 140 °C.

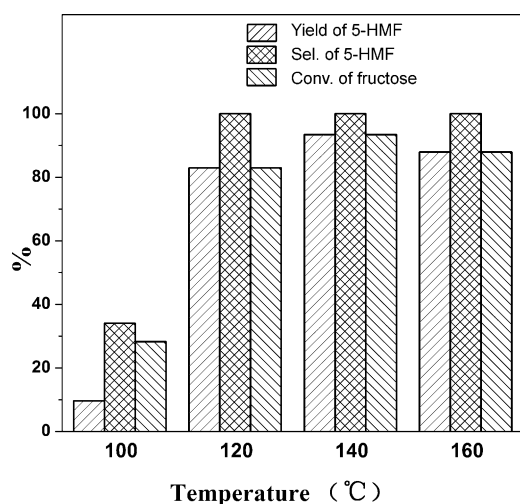


Figure 11. Effect of temperature on the dehydration of fructose to 5-HMF over CS-150; reaction conditions: 200 mg of fructose, 30 mg of CS-150, reaction time 30 min.

ing the reaction temperature improved the conversion of fructose to 5-HMF. The maximum 5-HMF yield of 93% with full fructose conversion was obtained at 140 °C; no further appreciable improvement in the yield was obtained upon further increasing the temperature to 160 °C. On the contrary, increasing the temperature further led to a slightly reduced 5-HMF yield, which indicated that CS-150 could catalyze 5-HMF degradation at higher reaction temperatures. Therefore, the optimum reaction conditions are 200 mg of fructose and 30 mg of CS-150 catalyst at 140 °C for 30 min.

Heterogeneous acid catalysts are advantageous owing to easy recovery from the reaction medium. Thus, apart from good catalytic activity, reusability is an important criterion for the solid catalysts. To demonstrate the reusability of the CS-150 catalyst for the dehydration of fructose to 5-HMF, the catalyst was separated by centrifugation, washed with deionized water, and dried at 80 °C; a three-cycle experiment was performed. Figure 12 shows the results of four successive reac-

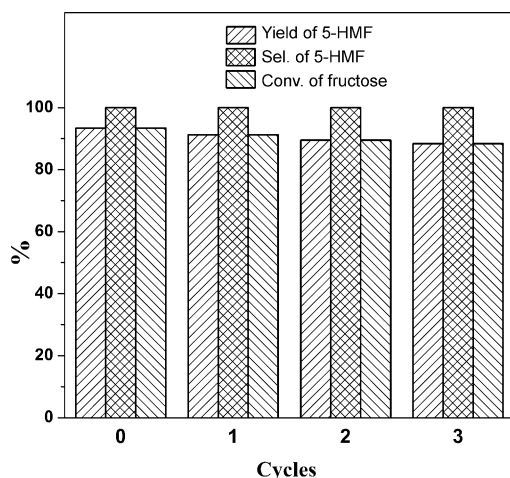


Figure 12. Reusability tests for the CS-150 catalyst; reaction conditions: 200 mg of fructose, 30 mg of CS-150, reaction time 30 min at 140 °C.

tions, and it can be observed that the catalytic activity was well maintained, and only a slight decline in selectivity and yield of 5-HMF was observed. After a three-cycle experiment, the 5-HMF yield was still nearly 90%. The elemental compositions, BET surface areas, I_D/I_G values from the Raman spectra, and acid-site densities of the CS-150 catalyst after three cycles were measured and the results are shown in Table 1. The results reveal that the BET surface area ($8.7 \text{ m}^2 \text{ g}^{-1}$), I_D/I_G value (0.81), percentage of sulfur component, and acid-site density are almost unchanged for the used CS-150 catalyst. Thus, the CS-150 catalyst does not interact with DMSO under at 140 °C. In addition, the results of thermal decomposition experiments also show that the CS catalysts are stable below 206 °C in air (Figure 4). So, the $-\text{SO}_3\text{H}$ groups on the surface of the CS-150 catalyst are not decomposed at 140 °C. Thus, the CS-150 catalyst has higher stability for the dehydration of fructose to 5-HMF with much higher activity.

To investigate the relationship between activity and acid density, the catalytic activities were also evaluated over the CS-130 and CS-170 catalysts, as shown in Figure S7 in the Supporting Information. The results show that the conversion of fructose is nearly 100%; however, the yield of 5-HMF is slightly different: 90.1, 93.3, and 89.1% for the CS-130, CS-150, and CS-170 catalysts, respectively. Figure 13 shows a plot of the yield of 5-HMF versus the acid density for the CS catalysts in Table 1. It further provides deeper insight into the relationship between the catalyst structure and performance, showing a striking linearity between the yield of 5-HMF and the total acid density of the CS catalysts. These results can also prove the surface acids are the active acid sites for the dehydration of fructose to 5-HMF under these reaction conditions. Several heterogeneous catalytic materials have been developed for the dehydration of fructose to 5-HMF, including ion-exchange resin, metal oxides, zeolites, sulfonic acid functionalized carbon materials ($\text{C}-\text{SO}_3\text{H}$), and MOF- SO_3H .^[14,26,28] Among these catalysts, CNT-PSSA, CNF-PSSA, CMK-5-BSA, and CNT-BSA showed good catalytic activity for fructose dehydration to 5-HMF, in which the highest yield of 5-HMF was 89% under optimal conditions over the CNT-PSSA catalyst.^[14] For the MOF- SO_3H catalyst, the highest yield of 5-HMF under optimal conditions

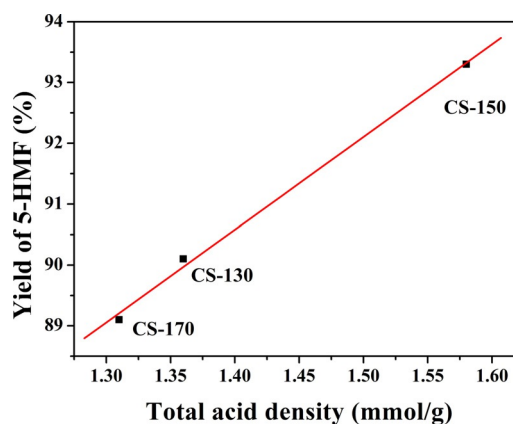


Figure 13. Relationship between yield of 5-HMF and total acid density for the CS catalysts.

reached 90%.^[26] Compared with the above catalysts, the CS-150 catalyst in our study showed excellent activity for fructose dehydration to 5-HMF: 93% yield of 5-HMF could be obtained at 140 °C in 30 min. Moreover, the CS-150 catalyst has the advantage of high stability, good recycling capabilities, low cost, and a facile preparation method.

Conclusion

The CS catalysts were prepared by a facile direct simultaneous carbonization and sulfonation method by using glucose and concentrated sulfuric acid as raw materials without the need for a hydrothermal process. The carbonization and sulfonation temperature played an important role among various synthesis conditions on carbon-based solid acid catalysts with high acid density. The optimal preparation conditions were a carbonization and sulfonation time of 20 min and a ratio of the amounts of glucose (g) to H₂SO₄ (mL) of 1:6 at 150 °C. The characterization results showed that the CS catalysts contained amorphous carbon with a high -SO₃H acid density. The CS-150 sample exhibited excellent catalytic properties for the transesterification of tributyrin with methanol owing to its high acid-site density; 97.8% selectivity and 97.2% yield of methyl butyrate were obtained, which corresponded to 99.4% conversion of tributyrin. The results displayed good linearity between the yield of methyl butyrate and the total acid density for fresh CS-170, CS-130, and CS-150 catalysts and used CS-150 catalyst. In addition, the dehydration of fructose to 5-HMF was also evaluated over the CS-150 catalyst, and a maximum 5-HMF yield of 93% with full fructose conversion (100%) was obtained. Moreover, the CS-150 catalyst had high stability with much higher activity for the dehydration of fructose to 5-HMF. There was also good linearity between the yield of 5-HMF and the total acid density for the CS catalysts.

Experimental Section

Catalyst preparation

The CS catalysts were prepared by a one-pot facile method of direct simultaneous carbonization and sulfonation with glucose and concentrated sulfuric acid (98% H₂SO₄). In brief, H₂SO₄ (20–40 mL) was added to glucose (5.00 g) in a 250 mL three-necked flask. The mixture was stirred for 0–60 min at different temperatures (130, 150, and 170 °C) in air, and the solid was separated by filtration. The obtained solid product was washed thoroughly with hot distilled water (about 80 °C) until neutral pH and no SO₄²⁻ in the filtrate was measured by the formation of BaSO₄ precipitate upon the addition of Ba(NO₃)₂ and a dilute solution of HNO₃. Finally, the obtained CS samples were dried at 80 °C for 12 h.

Catalyst characterization

XRD patterns of the catalysts were obtained with a D/MAX-3B X-ray diffractometer (Rigaku Co.) by using Cu_{Kα} radiation combined with a Ni filter. Raman measurements were recorded on a Jobin-Yvon HR800 spectrometer (laser λ = 459.9 nm). The FTIR spectra were recorded on a PE Spectrum One FTIR spectrometer as KBr disks at room temperature. The C, H, and S contents were analyzed

by combustion in a VarioMICROV1.9.0 elemental analyzer equipped with a TCD detector. The total acid-site density was estimated by acid–base titration: the CS catalyst (0.100 g) was added to a saturated aqueous solution of NaCl (20 mL) with ultrasonic treatment for 2 h. The mixture was separated by filtration and the filtrate was titrated with a 50 mmol L⁻¹ solution of KOH. The CA values were measured on a G-1erma, Kyowa Company, Japan, instrument.

Catalytic reaction evaluation

Transesterification reactions

All catalytic experiments were performed in a 30 mL double-layered glass reactor equipped with a reflux condenser, a magnetic stirrer, and a superthermostat, as previously described.^[25] Standard conditions were as follows: tributyrin (1.00 mL, 3.42 mmol) and methanol (17.1–102.4 mmol) were added to the flask. After the mixture was heated to the desired temperature (313–353 K), catalyst (5–40 mg) was added, and then the reaction was performed under these conditions for 4–8 h. The liquid products were analyzed quantitatively by GC (SP-2100 P.R. China, FID detector) with an OV-1 capillary column (30 m × 0.25 mm × 0.33 μm) by using calibration curves and cyclohexanone as an internal standard, according to a procedure reported in the literature.^[25] The yield of methyl butyrate was defined as the number of moles of methyl butyrate produced divided by the number of moles of tributyrin reacted divided by three (since three moles of methyl butyrate are produced per mole of tributyrin at complete conversion).

Fructose conversion into 5-HMF

In a typical run, the procedure for fructose dehydration was as follows: fructose (200 mg), CS-150 catalyst (10–50 mg), and DMSO (20 mL) were added to a 100 mL three-necked flask. The mixture was heated at 100–150 °C with vigorous stirring for 15–45 min. After the reaction, the mixture was recovered by centrifugation and then decanted into a volumetric flask by using pure water as the diluent. The mixture was analyzed by HPLC. The quantitative analysis of fructose was monitored by using a HPLC instrument (Shimadzu 20A) equipped with a refractive index detector and a Bio-Rad Aminex HPX-87H column. The 5-HMF product was analyzed by using a HPLC instrument (DIONEX Ultimate 3000) with an InterSustain C18 column and a λ = 284 nm UV detector.

Acknowledgements

This study is supported by the Major Foundation of Educational Commission of Heilongjiang Province of China (11531Z11), the Foundation of Educational Commission of Heilongjiang Province of China (11531286), the Postdoctoral Science-Research Developmental Foundation of Heilongjiang Province of China (LBH-Q12022), the Innovative Research Team in Heilongjiang University (Hdtd2010-10), and the Program for Innovative Research Team in University (IRT-1237). We also thank the Project Sponsored by the Scientific Research Foundation for the Returned Overseas Chinese Scholars, State Education Ministry (2013-1792), and Ministry of Human Resources and Social Security (2013-277).

Keywords: acid catalyst • dehydration • heterogeneous catalysis • sulfur • transesterification

- [1] a) J. R. Sohn, D. C. Shin, *Appl. Catal. B* **2008**, *77*, 386–394; b) W. L. Xie, L. L. Zhao, *Fuel* **2013**, *103*, 1106–1110; c) A. Daştan, A. Kulkarni, B. Török, *Green Chem.* **2012**, *14*, 17–37; d) S. K. Jana, P. Wu, T. Tatsumi, *J. Catal.* **2006**, *240*, 268–274.
- [2] a) F. Su, Y. H. Guo, *Green Chem.* **2014**, *16*, 2934–2957; b) N. Boza, N. Dergirmenbasi, D. M. Kalyon, *Appl. Catal. B* **2015**, *165*, 723–730; c) B. Saha, M. M. Abu-Omar, *Green Chem.* **2014**, *16*, 24–38; d) T. F. Wang, M. W. Nolte, B. H. Shanks, *Green Chem.* **2014**, *16*, 548–572.
- [3] a) Zillillah, G. Tan, Z. Li, *Green Chem.* **2012**, *14*, 3077–3086; b) K. Nakajima, M. Hara, *ACS Catal.* **2012**, *2*, 1296–1304; c) L. L. Xu, W. Li, J. L. Hu, K. Li, X. Yang, F. Y. Ma, Y. N. Guo, X. D. Yu, Y. H. Guo, *J. Mater. Chem.* **2009**, *19*, 8571–8579.
- [4] a) N. A. S. Ramli, N. A. S. Amin, *Appl. Catal. B* **2015**, *163*, 487–498; b) M. Kouzu, A. Nakagaito, J. Hidaka, *Appl. Catal. A* **2011**, *405*, 36–44; c) Y. H. Feng, B. Q. He, Y. H. Cao, J. X. Li, M. Liu, F. Yan, X. P. Liang, *Bioresour. Technol.* **2010**, *101*, 1518–1521; d) A. Takagaki, C. Tagusagawa, K. Domen, *Chem. Commun.* **2008**, 5363–5365; e) F. H. Alhassan, U. Rashid, Y. H. Taufiq-Yap, *Fuel* **2015**, *142*, 38–45; f) V. V. Ordonsky, V. L. Sushkevich, J. C. Schouten, J. van der Schaaf, T. A. Nijhuis, *J. Catal.* **2013**, *300*, 37–46; g) R. Weingarten, Y. T. Kim, G. A. Tompsett, A. Fernández, K. S. Han, E. W. Hagaman, Wm. Curt Conner Jr., J. A. Dumesic, G. W. Huber, *J. Catal.* **2013**, *304*, 123–134.
- [5] a) F. H. Alhassan, R. Yunus, U. Rashid, K. Sirat, A. Islam, H. V. Lee, Y. H. Taufiq-Yap, *Appl. Catal. A* **2013**, *456*, 182–187; b) A. Drelinkiewicz, Z. Kalembe-Jaje, E. Lalik, A. Zięba, D. Mucha, E. N. Konyushenko, J. Stejskal, *Appl. Catal. A* **2013**, *455*, 92–106; c) X. M. Liu, H. Y. Ma, Y. Wu, C. Wang, M. Yang, P. F. Yan, U. Welz-Biermann, *Green Chem.* **2011**, *13*, 697–701; d) R. Sheikh, M. S. Choi, J. S. Im, Y. H. Park, *J. Ind. Eng. Chem.* **2013**, *19*, 1413–419.
- [6] M. Hara, T. Yoshida, A. Takagaki, T. Takata, J. N. Kondo, S. Hayashi, K. Domen, *Angew. Chem. Int. Ed.* **2004**, *43*, 2955–2958; *Angew. Chem.* **2004**, *116*, 3015–3018.
- [7] a) M. Toda, A. Takagaki, M. Okamura, J. N. Kondo, S. Hayashi, K. Domen, M. Hara, *Nature* **2005**, *438*, 178; b) J. H. Zhang, L. F. Jiang, *Bioresour. Technol.* **2008**, *99*, 8995–8998.
- [8] M. Okamura, A. Takagaki, M. Toda, J. N. Kondo, T. Tatsumi, K. Domen, M. Hara, S. Hayashi, *Chem. Mater.* **2006**, *18*, 3039–3045.
- [9] S. Suganuma, K. Nakajima, M. Kitano, D. Yamaguchi, H. Kato, S. Hayashi, M. Hara, *J. Am. Chem. Soc.* **2008**, *130*, 12787–12793.
- [10] J. M. Fraile, E. García-Bordejé, L. Roldán, *J. Catal.* **2012**, *289*, 73–79.
- [11] X. H. Qi, H. X. Guo, L. Y. Li, R. L. Smith Jr., *ChemSusChem* **2012**, *5*, 2215–2220.
- [12] J. Y. Ji, G. h. Zhang, H. Y. Chen, S. L. Wang, G. L. Zhang, F. B. Zhang, X. B. Fan, *Chem. Sci.* **2011**, *2*, 484–487.
- [13] F. J. Liu, J. Sun, L. F. Zhu, X. J. Meng, C. Z. Qi, F. S. Xiao, *J. Mater. Chem.* **2012**, *22*, 5495–5502.
- [14] R. L. Liu, J. Z. Chen, X. Huang, L. M. Chen, L. L. Ma, X. J. Li, *Green Chem.* **2013**, *15*, 2895–2903.
- [15] a) B. L. Oliveira, V. T. da Silva, *Catal. Today* **2014**, *234*, 257–263; b) E. Lam, J. H. T. Luong, *ACS Catal.* **2014**, *4*, 3393–3410.
- [16] S. Paul, S. Ghosh, P. Bhattacharyya, A. R. Das, *RSC Adv.* **2013**, *3*, 14254–14262.
- [17] A. C. Ferrari, J. C. Meyer, V. Scardaci, C. Casiraghi, M. Lazzeri, F. Mauri, S. Piscanec, D. Jiang, K. S. Novoselov, S. Roth, A. K. Geim, *Phys. Rev. Lett.* **2006**, *97*, 187401.
- [18] Z. J. Xu, D. H. Cai, Z. H. Hu, L. H. Gan, *Microporous Mesoporous Mater.* **2014**, *195*, 36–42.
- [19] B. Garg, T. Bisht, Y. C. Ling, *RSC Adv.* **2014**, *4*, 57297–57307.
- [20] a) M. G. Goesten, J. Juan-Alcañiz, E. V. Ramos-Fernandez, K. B. S. S. Gupta, E. Stavitski, H. V. Bekkum, J. Gascon, F. Kapteijn, *J. Catal.* **2011**, *281*, 177–187; b) A. Osatiashtiani, A. F. Lee, D. R. Brown, J. A. Melero, G. Morales, K. Wilson, *Catal. Sci. Technol.* **2014**, *4*, 333–342.
- [21] P. A. Russo, M. M. Antunes, P. Neves, P. V. Wiper, E. Fazio, F. Neri, F. Barreca, L. Mafra, M. Pillinger, N. Pinna, A. A. Valente, *J. Mater. Chem. A* **2014**, *2*, 11813–11824.
- [22] a) J. P. Dacquain, H. E. Cross, D. Robert Brown, T. Düren, J. J. Williams, A. F. Lee, K. Wilson, *Green Chem.* **2010**, *12*, 1383–1391; b) C. Pirez, A. F. Lee, C. Jones, K. Wilson, *Catal. Today* **2014**, *234*, 167–173; c) F. J. Liu, A. M. Zheng, I. Noshadi, F. S. Xiao, *Appl. Catal. B* **2013**, *136*, 193–201.
- [23] a) Q. Shu, J. X. Gao, Z. Nawaz, Y. H. Liao, D. Z. Wang, J. F. Wang, *Appl. Energy* **2010**, *87*, 2589–2596; b) Q. Shu, Z. Nawaz, J. X. Gao, Y. H. Liao, Q. Zhang, D. Z. Wang, J. F. Wang, *Bioresour. Technol.* **2010**, *101*, 5374–5384.
- [24] a) Y. H. Zu, G. Liu, Z. L. Wang, J. H. Shi, M. Zhang, W. X. Zhang, M. J. Jia, *Energy Fuels* **2010**, *24*, 3810–3816; b) D. Kusdiana, S. Saka, *Fuel* **2001**, *80*, 693–698; c) H.-Y. Shin, S.-H. An, R. Sheikh, Y. Ho Park, S.-Y. Bae, *Fuel* **2012**, *96*, 572–578; d) S. L. Yan, S. O. Salley, K. Y. Simon Ng, *Appl. Catal. A* **2009**, *353*, 203–212.
- [25] a) X. Y. Niu, C. M. Xing, W. Jiang, Y. L. Dong, F. L. Yuan, Y. J. Zhu, *Reac. Kinet. Mech. Catal.* **2013**, *109*, 167–179; b) W. Jiang, X. Y. Niu, F. L. Yuan, Y. J. Zhu, H. G. Fu, *Catal. Sci. Technol.* **2014**, *4*, 2957–2968.
- [26] J. Z. Chen, K. G. Li, L. M. Chen, R. L. Liu, X. Huang, D. Q. Ye, *Green Chem.* **2014**, *16*, 2490–2499.
- [27] Y. Roman-Leshkov, J. N. Cheda, J. A. Dumesic, *Science* **2006**, *312*, 1933.
- [28] a) X. Qi, M. Watanabe, T. M. Aida, R. L. Smith Jr., *Green Chem.* **2008**, *10*, 799; b) S. Dutta, S. De, A. K. Patra, M. Sasidharan, A. Bhaumik, B. Saha, *Appl. Catal. A* **2011**, *409–410*, 133–39; c) X. Tong, M. Li, N. Yan, Y. Ma, P. J. Dyson, Y. Li, *Catal. Today* **2011**, *175*, 524–527; d) P. Rivalier, J. Duhamet, C. Moreau, R. Durand, *Catal. Today* **1995**, *24*, 165–171.

Manuscript received: June 14, 2015
Final Article published: July 17, 2015